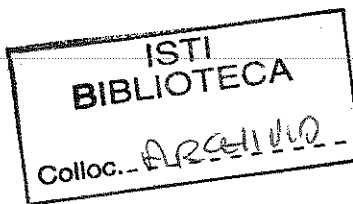


A3-10
2002



BEPPOSAX EQUATORIAL UNCONTROLLED RE-ENTRY

C. Portelli¹, L. Salotti¹, L. Anselmo², T. Lips³, A. Tramutola⁴

¹*Agenzia Spaziale Italiana, Viale Liegi 26, 00198 Rome, Italy*

²*Istituto di Scienza e Tecnologie dell'Informazione, CNR, Via G. Moruzzi 1, 56124, Pisa, Italy*

³*HTG - Hyperschall Technologie Göttingen, Max-Planck-Str. 19, 37191 Katlenburg-Lindau, Germany*

⁴*Alenia Spazio S.p.A., Strada antica di Collegno 253, 10146 Turin, Italy*

ABSTRACT

The X-ray astronomy satellite BeppoSAX (Satellite per Astronomia X, "Beppo" in honor of Giuseppe Occhialini), is a project of the Italian Space Agency (ASI) with the participation of the Netherlands Agency for Aerospace Programs (NIVR). BeppoSAX was launched by an Atlas G-Centaur directly into a circular 600 km orbit at 3.9 degrees inclination on April 30, 1996. The satellite is a three axis stabilized spacecraft with a total mass of about 1400 kg and main dimensions in flight configuration of about 2450 mm x 8980 mm x 3650 mm. The current (September 21, 2002) flight altitude is about 435 km and its uncontrolled re-entry is predicted late in 2002, or in 2003, with 26 kg of hydrazine on board that could not be vented or used for controlled re-entry due to the gyro package's total failure. Due to the relatively high mass of BeppoSAX, it must be expected that parts of the satellite will survive the re-entry into the Earth atmosphere. The Italian Space Agency has committed a study to analyse of the destructive phase of the uncontrolled atmospheric re-entry by means of a dedicated European software tool (SCARAB). The expected outputs will be used in order to determine how much of the spacecraft and how many fragments of it will reach the ground on the equatorial earth zone. This paper will address the peculiarities of the spacecraft's initial status, its risks at end of life, and the SCARAB modeling as well as its six dimension flight dynamics re-entry analysis results also in terms of the destruction history tree. Consideration will be made of the ground dispersion and casualty area due to the very restricted equatorial zone impacted.

BEPPOSAX DESIGN AND END OF LIFE STATUS

The satellite for X-ray Astronomy BeppoSAX, launched on April 30, 1996, was devoted to systematic, integrated and comprehensive studies of galactic and extra-galactic sources in the energy band 0.1-300 keV and was a joint venture of the Italian Space Agency (ASI) and the Netherlands Agency for Aerospace Programs (NIVR) with the participation of SRU/SRON and ESA SSD/ESTEC. The prime contractor for the space segment was Alenia Spazio/Turin while Telespazio S.p.A/Rome managed the ground segment.

BeppoSAX was de-activated by ground command on April 30, 2002, exactly 6 years after its launch.

During the in flight scientific activity the embarked instrumentation performed in excess of 12,500 observation sessions of celestial targets, providing the worldwide X-ray astronomy community more than 650 Gbytes of scientific data which were used to enlarge the knowledge of the X-ray sky and proved essential for the recent breakthrough in the Gamma Ray Burst astrophysics domain. The advancement in the Gamma Ray Burst field resulted in the assignment of the prestigious 'Bruno Rossi' prize by the American Astronomical Society to the BeppoSAX team in 1998.

The BeppoSAX spacecraft was designed to perform a scientific mission in a near circular low Earth orbit (600 -450 km) with an inclination of less than 4°. The Attitude and Orbit Control Subsystem (AOCS) was designed to bear disturbance torques up to a value estimated at about 1.32 Nms at 450 km of altitude. The AOCS was based on Sun sensors, magnetometers, gyroscopes, star-trackers and reaction wheel as actuators. The magnetic torquer assembly carried out the angular momentum unloading of the reaction wheels.

The original design of the AOC subsystem was based on gyroscopes (6 gyroscopes, 4 in hot redundancy and 2 in cold redundancy), which were used for attitude reference during slews and for controlling the attitude during scientific pointing with star-trackers obscured by the Earth's body. The gyroscopes were also used to extrapolate the magnetic vector between measurements and the Sun vector during eclipses. In order to allow extensions of the scientific mission in case of orbital decay, a Reaction Control Subsystem (RCS), consisting of two redundant branches of six 11N-hydrazine thrusters and a fuel tank storing 26 kg of hydrazine, was installed on board. The propulsion, provided during a delta-V maneuver, allowed a maximum altitude boost of about 70 km via a Hohmann transfer. One other task of the RCS subsystem was the unloading of the reaction wheels momentum (Fast Unload Mode) in case of a high-level disturbance torque at low altitudes (≤ 450 km). Finally, the RCS subsystem was in charge of controlling the spacecraft in case of separation from the expendable launch vehicle with non-nominal angular momentum (> 13 Nms).

The correct injection in the operational orbit (600 km) with low angular momentum after separation did not require the support of the RCS; in addition, the low level of the external disturbance torques, experienced during the 6 years of operational life, never prompted the need of performing delta-V maneuvers.

Failures of the gyroscopes packages occurred during the first year on orbit and were solved with a progressive approach. Initially, a new AOC subsystem safe control mode was developed which was totally 'gyroless' (Gyroless Safe Mode). Then, a new attitude scientific control mode was provided which used only one gyro unit (Extended Science Mode 1, August 1997). Finally, after the failure of the last gyro, a totally "gyroless" SW version (ESM 2, November, 2001) for scientific observation was loaded on board and used up to the de-activation of the mission on April 30, 2002. All the modifications of the original AOC subsystem on board SW package were accommodated using the available resources (80C86 μ P, 128 Kb of RAM). In the process, it was decided to remove the original DVM because the execution of delta-V maneuvers without the usage of the full gyroscope package was not possible. This fact led, as a consequence, to the complete deactivation of the RCS subsystem on board.

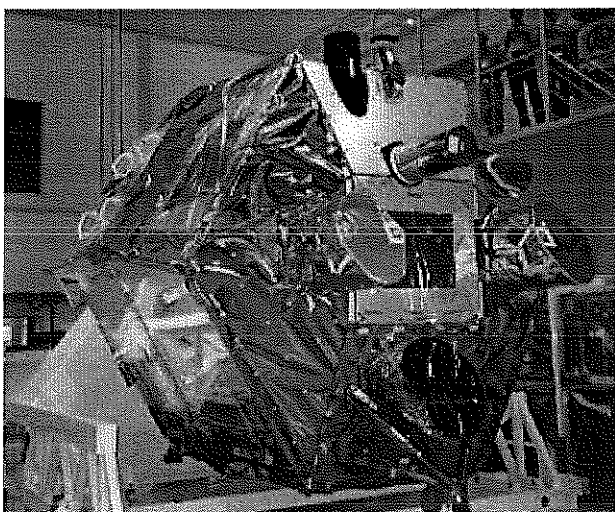


Fig. 1. BeppoSAX picture during AIV at system level

Therefore, the BeppoSAX design and its final configuration did not allow any controlled re-entry. This led ASI to identify a set of end-of-life rules, compliant with ESA standard ECSS-Q-40, to be applied for the dismissal of the mission. These rules were based on the need to avoid any open-loop maneuver that could cause an uncontrolled orbital change, as well as on the deactivation of the main subsystems reducing the energy level contained in each of them to the maximum extent. However, venting of the RCS tank was not feasible because no venting valves were present on board. On the other hand, venting of hydrazine through the Flow Control Valves would have caused an open loop full firing without AOC subsystem control.

The disposal passivation procedure eventually commanded the satellite in safe mode in order to allow the disabling of all the AOC and on board data handling autonomous re-configuration and to reduce the energy contained in the batteries inhibiting the recharging process. As a last step, the switch off of both main and redundant thermal control computers concluded the procedure and left BeppoSAX without power and thermal/attitude control. Even in this condition, the BeppoSAX satellite cannot be considered completely switched off, because the presence of sufficient sunlight on the solar arrays during the uncontrolled tumbling can power-on the OBDH and AOCS subsystems prompting their boots from PROMs. This power-on condition lasts for the time of sun illumination and is not able to resume attitude control due to the lack of the gyroscopes and the excessive angular momentum embarked. The final status of the satellite is therefore dynamically uncontrolled and toggles between a power-on and power-off status of the main subsystems, following the random sun illumination on the arrays.

BEPPOSAX MODELLING WITH SCARAB

SCARAB (Version 1.5), a software system developed by Hyperschall Technologie Göttingen (HTG) for the European Space Agency (ESA), has been used to model the satellite (Lips, 2002a) and also later to perform the re-entry analysis (Lips, 2002b). SCARAB is a multidisciplinary tool which allows modeling a re-entry object with all its important properties: detailed panelized geometry, extensive material database, material properties, mass, thermo-physical, and structural model (Fritsche, 1997 and 2000).

BeppoSAX has been modeled as close to reality as possible. Due to the very detailed documentation provided by the satellite manufacturer, this was possible down to the component level of each subsystem. If possible, all parts have been modeled with the actual wall thickness. Otherwise the wall thickness was adapted to the mass of the part (specified in the mass budget). In particular, all the electronic boxes have been modeled in this way: with the real outer dimensions, but with a constant wall thickness matching the mass of the electronic box.

The satellite has been modeled in flight configuration with a full RCS tank. This corresponds to the present configuration of the satellite in orbit.

The model consists of 859 “primitives” (basic geometric elements like spheres, boxes, plates (circular, rectangular, triangular), cylinders, cones). The geometric information of these primitives has been translated into a panelized model with 72,584 volume panels. In a last step each volume panel is transformed into surface panels. This yields 177,708 surface panels (see Figure 2 and 3).

The structural model consists of 6 “cuts” in order to analyze the stress in the hinges between each solar panel.

Also the RCS tank has been modeled, including its liquid contents, in order to analyze tank bursting.

A very accurate level of modeling has been achieved for BeppoSAX. Primarily, the total mass and the mass distribution of the model correspond almost exactly to the data of the real satellite. The total model mass difference is below 0.02% (model mass: 1,385.419 kg, real mass: 1,385.63 kg). The center of gravity location of the complete BeppoSAX model matches the actual center of gravity within a distance below 12 mm. The modeled moments of inertia agree within the following boundaries: $I_{xx} < 3.3\%$, $I_{yy} < 0.9\%$, $I_{zz} < 5.8\%$.

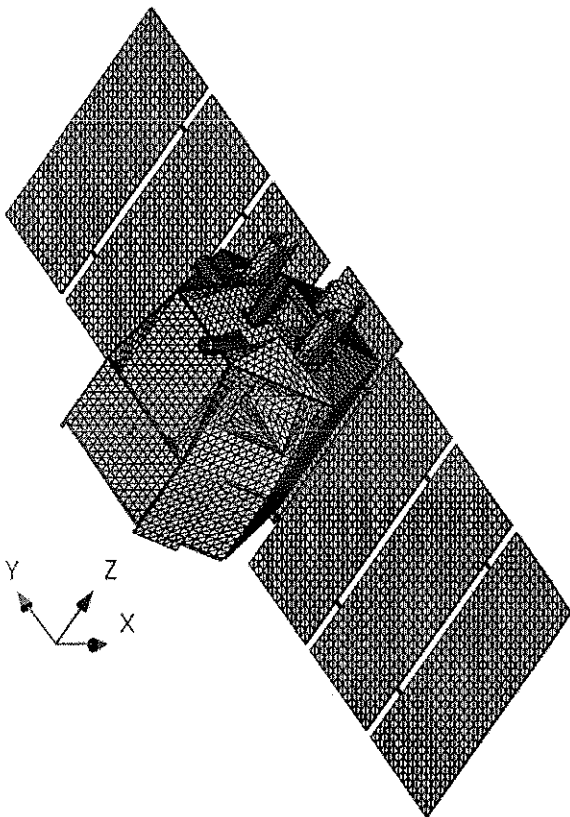


Fig. 2. SCARAB model of BeppoSAX

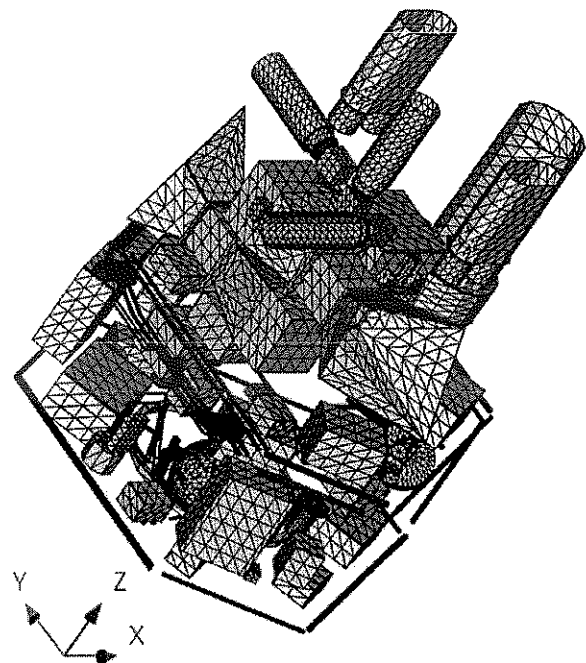


Fig. 3. SCARAB model of BeppoSAX without structure and solar panels

BEPPOSAX RE-ENTRY ANALYSIS WITH SCARAB

Initial Conditions

In order to start a re-entry analysis, the initial orbit and attitude conditions of the satellite have to be specified. The exact orbital parameters, right at the beginning of the re-entry, as well as the attitude and rotation of the satellite, are yet unknown. Therefore, they have been predicted based on the current orbital status of BeppoSAX, or arbitrary chosen to reasonable values (see Tables 1 and 2).

Semi major axis	6,830.876 km
Eccentricity	0.000559
Inclination	3.961°
Right ascension of ascending node	315.448°
Argument of perigee	195.444°
True anomaly	164.590°

Semi major axis	6,500 km
Eccentricity	0.000559
Inclination	3.961°
Right ascension of ascending node	0°
Argument of perigee	0°
True anomaly	0°

The estimated initial data correspond to a geodetic altitude of 118.228 km, an aerodynamic velocity of 7.362 km/s, and a flight path angle of $\approx 0^\circ$ (near horizontal re-entry). The initial attitude conditions have been arbitrarily set such that the x-axis of the satellite is aligned to the flight direction. The satellite is assumed not to rotate at the beginning of the re-entry.

Re-entry and Fragmentation History

During the re-entry the satellite fragments in several stages. After each fragmentation two or more fragments are produced which have to be treated as separate re-entry objects. Generally, there is one main object (the heaviest fragment) and smaller sub-fragments. The main object is the most important one because it may be the biggest fragment to reach the ground. In addition, the main object generates most of the sub-fragments, because sub-fragments mostly do not fragmentize again. They are relatively small and demise, or if they are big enough they reach ground.

In the following the results for the main object are presented in details.

Figure 4 shows the altitude history of the main object. Until the velocity of a re-entry object becomes lower than Mach number 6 a full 6 degrees of freedom (DoF) integration of the equation of motion is performed. Below Mach number 6 a 3 degrees of freedom analysis is conducted.

In Figures 4-10 the time axis indicates the seconds elapsed since the entry state in Table 2.

Figures 5 and 6 show the history of angle of attack and slip angle of the main object for a 6 DoF analysis. The main object rotates and oscillates mainly around the former y-axis of satellite combined with an overlaid oscillation around the former z-axis (x-axis in flight direction corresponds to 0° angle of attack and 0° bank angle).

Figure 7 shows the maximum heat flux on the main fragment. The peak maximum heat flux is about 774 kW/m² at an altitude of 57.5 km (2,067 s).

Figure 8 shows the maximum temperature of the main object. After 1,563 s a constant temperature of 883 K is reached. This temperature corresponds to the melting temperature of the aluminum alloy AA5052. It takes about 135 s until the temperatures of other materials become higher. The overall peak maximum temperature is about 1,723 K at an altitude of 65.9 km (2,029 s).

The mass of the main object is shown in Figure 9. This figure illustrates that the melting starts 1,667 s after the beginning of the calculation at an altitude of 99.1 km. Within 459 s the mass of the main fragments drops from 1,341.485 kg down to 119.877 kg. This is not the total mass reaching the ground, but only the mass of the biggest fragment. For the final masses of the other fragments see Table 4.

Present and further data have been calculated during the re-entry analysis. Together this yields 2.9 GB of data. The complete analysis has taken about 3 weeks (~3 Pentium III processors at 1.2 GHz).

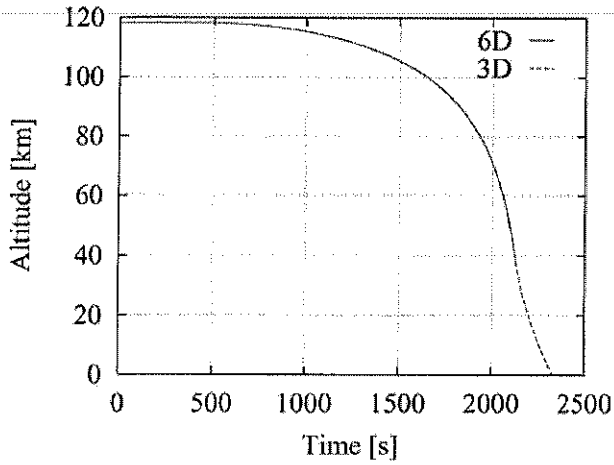


Fig. 4. Altitude history of the main object

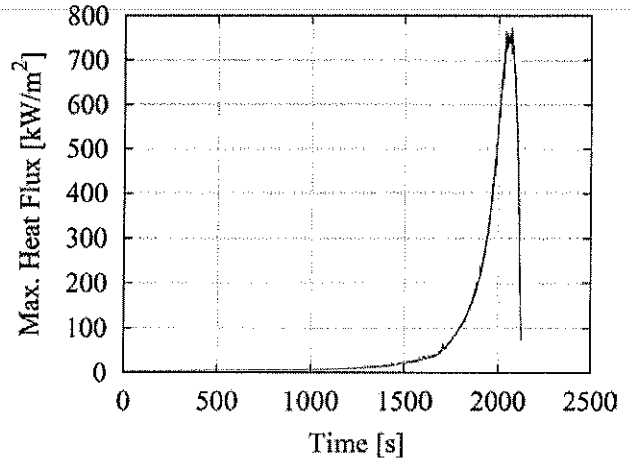


Fig. 7. Maximum heat flux history of the main object

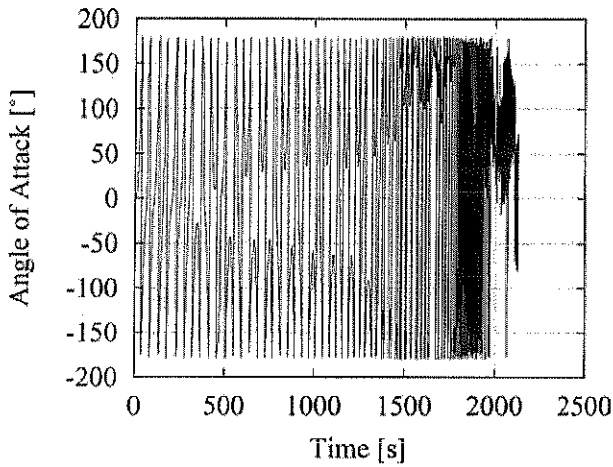


Fig. 5. Angle of attack history of the main object

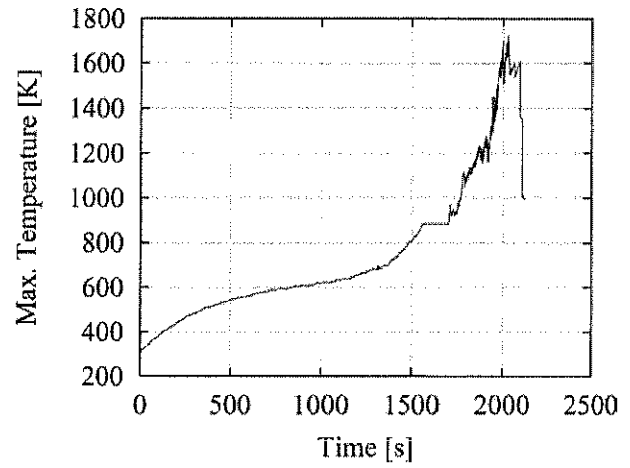


Fig. 8. Maximum temperature history of the main object

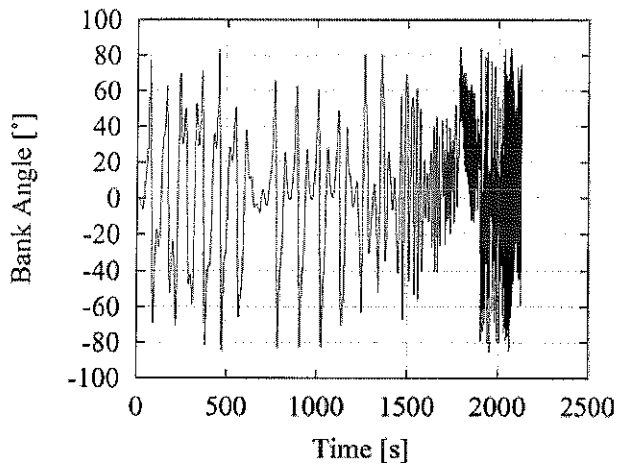


Fig. 6. Slip angle history of the main object

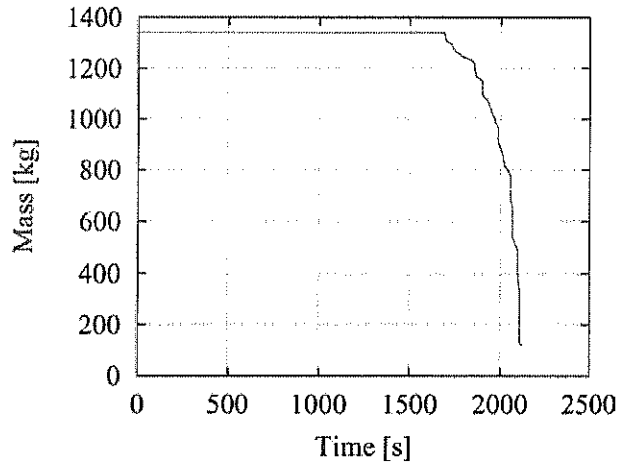
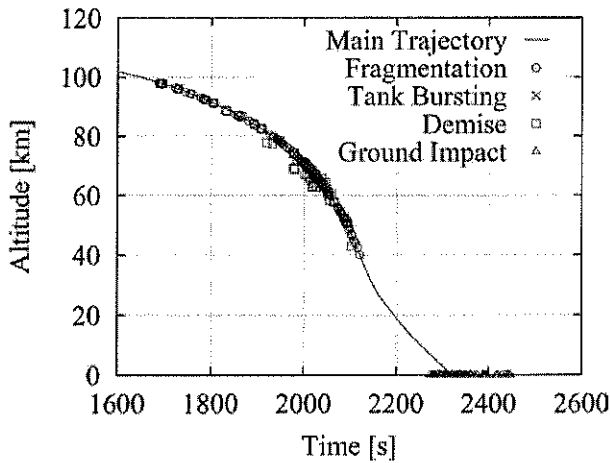


Fig. 9. Mass history of the main object

The fragmentation history describes all fragmentation events during the re-entry. Each fragment is tracked until it either fragments again, demises, or reaches the ground. Figure 10 shows the distribution of all the events along the main trajectory (trajectory of the main object). Table 3 includes the number of each event and the time and altitude range in which they have occurred.



Event	No.	Time range	Altitude
		[s]	range [km]
Fragmentation	85	1,687 – 2,121	98.2 – 40.0
Tank bursting	1	1853	87.5
Demise	87	1,690 – 2,103	98.0 – 43.0
Ground impact	42	2,273 – 2,447	0.0
Total	215	–	–

Fig. 10. BeppoSAX re-entry event distribution along the main trajectory.

Shortly after the first fragmentation event, the first demise event also occurs, because at the beginning of the re-entry only small fragments are generated. Demise stops some seconds before and some kilometers above the last fragmentation event. The last generated fragments reach ground without further fragmentation.

The fragmentation altitude range covers about 49% of the altitude range of the complete re-entry. This shows the important influence of shielding effects on exposure time and altitude for internal parts of the spacecraft.

Table 4 gives an overview for the 42 fragments reaching the ground. Each fragment is specified by a number, its name and material, mass, and mean cross-section area. Images of these fragments are shown in Figure 11.

No	Fragment	Mass [kg]	Area [m ²]	No.	Fragment	Mass [kg]	Area [m ²]
1	Solar panel bracket; A	0.204	0.003	22	Tape recorder unit; Al	5.648	0.038
2	Battery ; Al	14.927	0.083	23	Thruster block, pipe; ©	1.395	0.026
3	Scientific payload; ®	71.683	0.250	24	Support structure; Ti	0.420	0.007
4	Support structure; Ti	0.699	0.014	25	Support structure; Ti	0.420	0.007
5	Power distribution unit; Al	6.270	0.084	26	Thruster block, pipe; ©	1.357	0.026
6	Empty Tank – Ti	5.524	0.160	27	Scientific payload; (*)	59.721	0.480
7	Power protection unit; Al	5.774	0.084	28	Scientific payload; (*)	60.721	0.481
8	Thermal control unit; Al	29.861	0.183	29	Support Structure; Al	0.008	0.000
9	Pipe Segment; Ti	0.116	0.013	30	Support Structure; Al	0.009	0.000
10	Pipe Segment; Ti	0.099	0.014	31	Reaction wheel, electr.; ©	14.607	0.146
11	Pipe Segment; Ti	0.118	0.012	32	Reaction wheel; ©	5.579	0.046
12	Pipe Segment; Ti	0.086	0.012	33	Thrust cone (structure); Al	12.508	0.336
13	Pipe Segment; Ti	0.065	0.012	34	Scientific payload; ®	92.779	0.221
14	Thrusters with pipe; ©	0.720	0.017	35	Scientific payload; ®	72.138	0.253
15	Thrusters with pipe; ©	0.704	0.018	36	Support structure; Al	0.371	0.033
16	Harness; Cu	2.735	0.019	37	Magnetic torquer; Cu	1.788	0.018
17	Harness; Cu	3.060	0.019	38	Support structure; ®	2.399	0.018
18	Harness; Cu	8.792	0.047	39	Reaction wheel, electr.; ®	10.573	0.146
19	Dummy/balance mass; Al	11.135	0.071	40	Reaction wheel, electr.; ®	15.956	0.149
20	Dummy/balance mass; Al	11.342	0.029	41	Main object; (® +Cu)	119.887	0.868
21	Support structure; Al	0.004	0.000	42	Main bus unit; Al	4.306	0.036

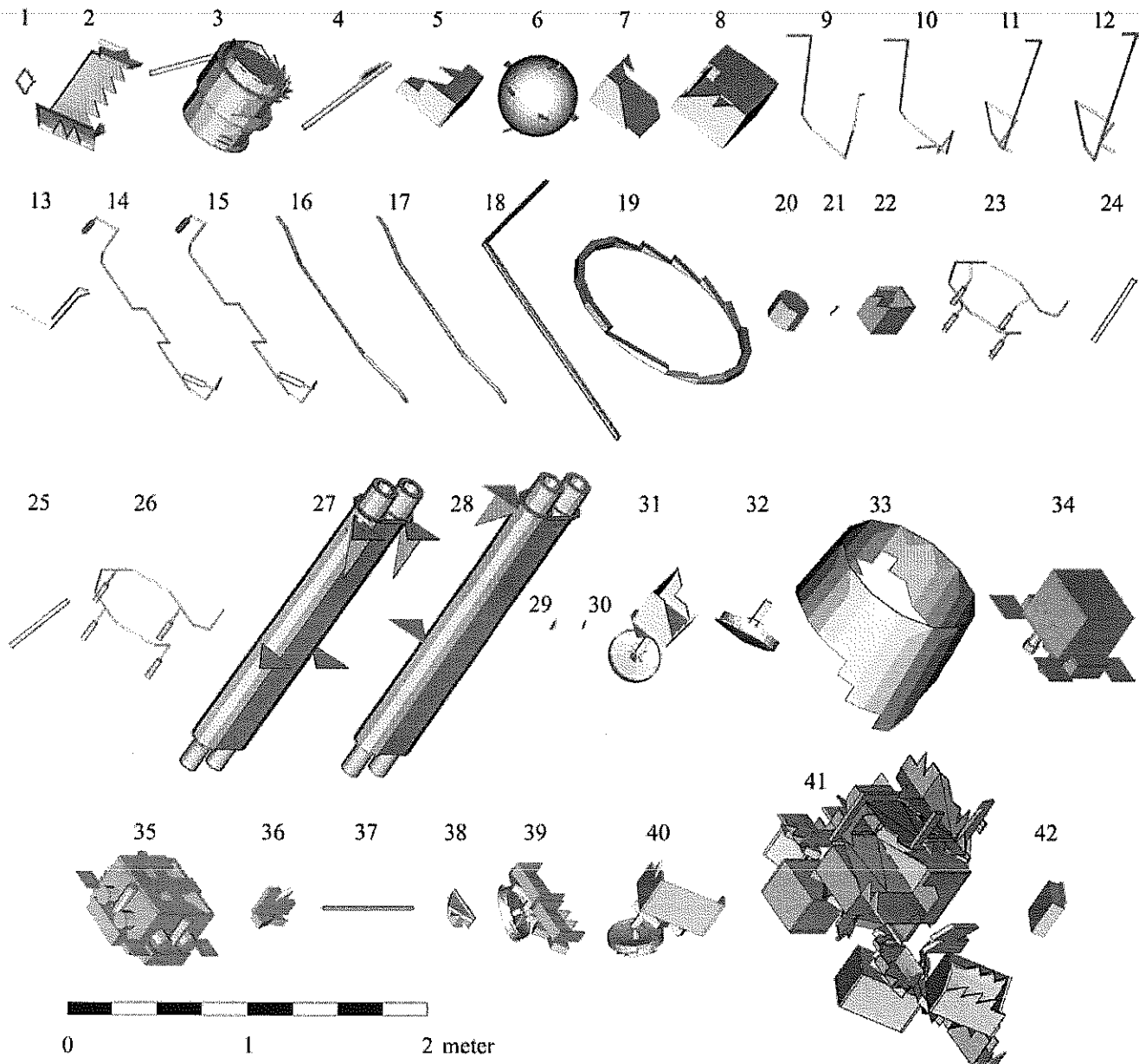


Fig. 11. Ground impact fragments of BeppoSAX.

Material symbols in table 4: A = Inconel or A316; Al= Aluminum alloy; Cu = Copper; Ti = Titanium alloy; (*) = CFRP, Titanium alloy, A316, Invar, Copper and Aluminum alloy; ® = Aluminum alloy, Titanium alloy, © = Inconel or A316, Aluminum alloy.

Altogether, 42 fragments of BeppoSAX are assumed to reach the ground with a total mass of 656.226 kg. This corresponds to 48.92% of the initial mass at the beginning of the calculation (1,341.485 kg). The small difference of 43.934 kg (3.17%) between the total mass at the beginning of the calculation and the total model mass, results from the panelizing of the geometry.

The fragment dispersion on ground is shown in Figure 12. All the fragments are spread out over an area of about 10,500 km² (315.3 x 33.3 km). The impacts take place close to the ground track of the main object.

The impact velocities vary between 16.9 and 128.6 m/s (60.9 and 462.8 km/h). Figure 13 shows the impact velocities of the fragments versus their mass to area ratio. It is shown that the impact velocity of a fragment corresponds with its aerodynamic free fall velocity. Analytic solutions for constant drag coefficients C_D between 0.3 and 0.6 are also shown. The fragments impact on the ground vertically.

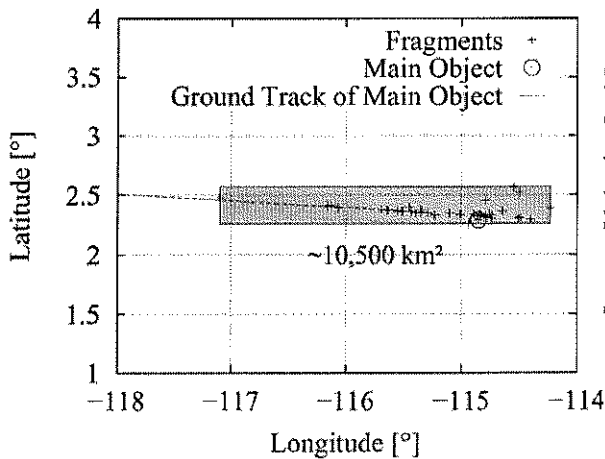


Fig. 12. Ground dispersion of fragments

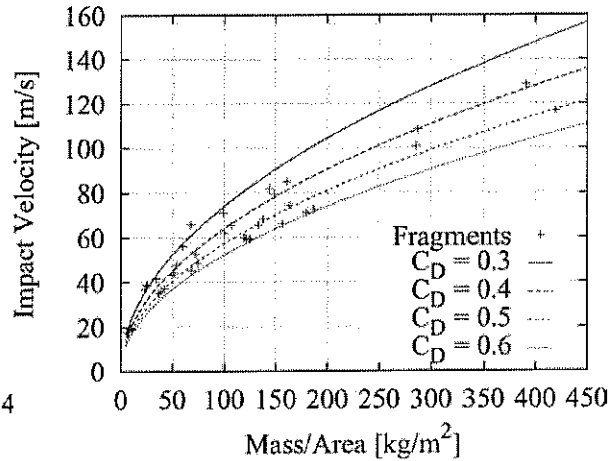


Fig. 13. Impact velocities of fragments

BEPOSAX PRELIMINARY ON GROUND RISK ANALYSIS

Casualty Area

The casualty area D_A has been defined by NASA (1995). It indicates the ground risk for human casualties and is calculated as follows:

$$D_A = \sum_i (0,6 + \sqrt{A_i})^2 \quad (1)$$

Where A_i is the cross-section area of each fragment in square meters.

The NASA Safety Standard (NASA, 1995) requires that the casualty area for an uncontrolled re-entry shall not exceed 8 m². The casualty area for all the ground impact fragments listed in Table 4 is calculated to be 32.419 m².

The mass distribution histogram in Figure 14 and the diagram of the casualty area of fragments vs. mass in Figure 15 show that most of the fragments (36) are heavier than 0.1 kg. But even the smallest fragments would each contribute as minimum of 0.36 m² to the total casualty area although they pose a lower risk (impact velocity below 40 m/s, kinetic energy below 20 Joule).

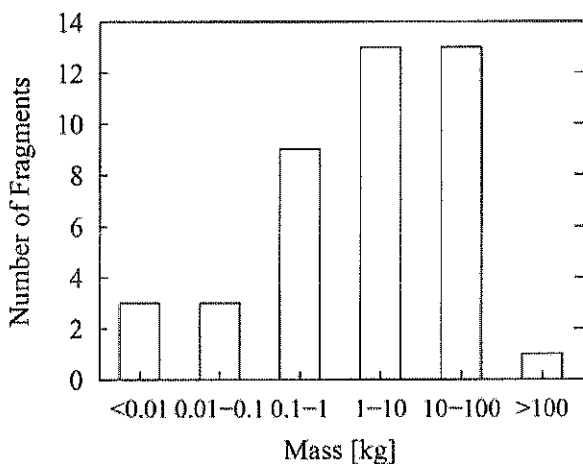


Fig.14. Mass distribution histogram

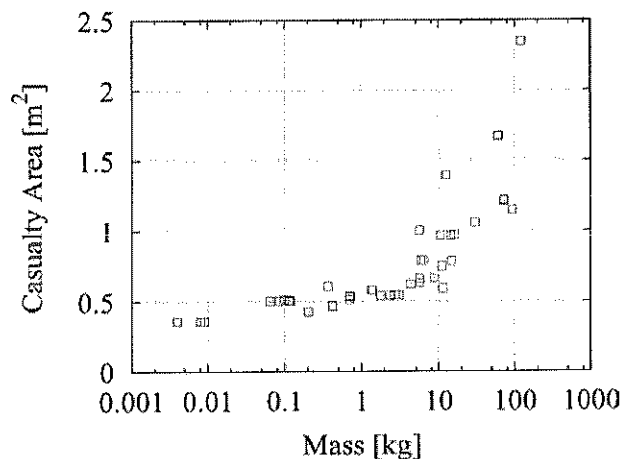


Fig. 15. Casualty area of fragments vs. mass

If, fragments smaller than 0.1 kg are neglected, the casualty area is calculated to be 29.816 m².

In order to evaluate the associated risk on ground, a precise decay analysis should be done including updates of solar and geomagnetic activity data and the attitude loss after passivation (from April 30, 2002). The predictions would finally permit ASI to determine the ground impact longitude band in order to issue warning messages.

A preliminary assessment was made to evaluate the human injury risk in the equatorial band that includes all territories within ± 4 degrees of latitude. In order to perform such a preliminary evaluation, a subset of 1990 global population data ($1^\circ \times 1^\circ$ Longitude/Latitude resolution) has been extracted from an Internet database (UNEP, 1990). 799 out of 2,880 (=27.74%) of the $1^\circ \times 1^\circ$ population bins in the $\pm 4^\circ$ latitude band were populated.

Moreover to simplify the computation, no augmentation factor (for sliding, re-bounce, etc.) was considered and a uniform probability distribution with latitude band was considered.

In spite of the large part of the longitude band covered by ocean (72.26%), the computation of average human injury probability resulted in $\approx 1/5,200$, which is almost a factor of 2 above the recommended threshold defined by NASA (1995).

Reentry Predictions

BeppoSAX is now subjected to a significant air drag, which will lead quite soon to its reentry into the denser layers of the atmosphere. The high level of solar activity still recorded two and half years after the nominal maximum of the current solar cycle will probably result in an earlier reentry date between January and March 2003. However, a longer residual lifetime cannot be ruled out yet, depending on the evolution of the solar activity in the coming months.

As explained at the beginning of this paper, the satellite cannot be maneuvered anymore, so its orbital decay and final plunge to the Earth will be totally uncontrolled. However, ASI has decided to maintain a reduced monitoring capability of the spacecraft orbital evolution, trying to make reasonable predictions of the reentry date and, if possible, a post-reentry assessment to formally close the mission. The first task of the proposed activity will be the study of the evolution of the BeppoSAX ballistic coefficient ($B = C_D A/M$) after the mission de-activation on April 30, 2002 (C_D is the drag coefficient, A the satellite average cross-section and M the mass). The value observed during the operational scientific mission was quite stable over long periods of time and varying solar activity conditions ($B \cong 0.03 \text{ m}^2/\text{kg}$), but in the new orbital (lower altitude) and dynamical (the attitude is not controlled anymore) regime, the ballistic coefficient may be significantly different and not necessarily stable. This information is crucial to obtain realistic reentry predictions and may provide useful hints concerning the rotational state of the spacecraft.

Since the satellite has been de-activated and the ground station in Malindi (Kenya) is no longer operational, the only source of orbital data will be the NORAD two-line elements (TLE) provided by the NASA Orbital Information Group, at the Goddard Space Flight Center. The historical data sets already archived and periodically updated are sufficient for the ballistic coefficient analysis, but the timely availability of new TLE will be critical for meaningful reentry predictions close to the reentry date.

Unfortunately, due to the orbital geometry (very low inclination) and to the decreasing altitude, the coverage of the American military sensors will not be good and significant gaps in the TLE availability could occur during the critical few days of residual lifetime. In spite of this, ISTI may use the available state vectors to monitor the satellite decay, periodically recalibrate the ballistic coefficient and issue updated reentry predictions with the associated uncertainties (windows).

Due to the intrinsic uncertainties of an uncontrolled reentry (solar and geomagnetic activity, air drag modeling, spacecraft rotational status, drag coefficient, etc.), it will be practically impossible to sort out a subset of orbit tracks during which the final plunge into the denser layers of the atmosphere will probably occur, until one or two days before the event. Moreover, due to the orbit geometry, the areas of potential interest for the fall of the surviving fragments will be compressed in the ± 4 degree latitude band and basically none of the countries lying in the equatorial belt might be excluded from the reentry window before the satellite disintegration in the Earth atmosphere.

Assuming a steady flux of TLE available during the last two days of the satellite lifetime, one could try to identify the subset of specific sub-satellite tracks included in the progressively shrinking reentry windows, in order to verify, if large cities and/or densely populated areas might be affected or not by the fall of the surviving BeppoSAX fragments.

Finally, a post-reentry assessment will be carried out using the additional orbital data eventually issued by NORAD through NASA, in order to better pinpoint the area of debris fall. This activity will be particularly important in the quite probable case that no direct sighting or witness account of the reentry is reported.

CONCLUSIONS

This paper summarizes an analysis of the re-entry survivability of parts of the BeppoSAX satellite and the assessment of resulting risk on ground. The spacecraft design did not include the management of the disposal phase.

The analysis results have shown that a leak before burst of the RCS fuel tank is highly probable. This event will occur below 90 km therefore limiting the risk to other space systems from its breakup.

The casualty risk on ground, higher than 1/10,000, is clearly due to the very tight latitude band associated with the satellite inclination and the spacecraft design materials (several elements in titanium).

The Italian Space Agency has now included the disposal phase as a standard on all its contracts.

REFERENCES

- Fritsche, B., G. Koppenwallner, T. Roberts, et al., Spacecraft Disintegration during Atmospheric Re-entry, Executive Summary, ESOC Contract No. 11427/95/D/IM, HTG-Report-97-6, HTG – Hyperschall Technologie Göttingen, Katlenburg-Lindau, Germany, 1997.
- Fritsche, B., G. Koppenwallner, M. Ivanov, et al., Advanced Model for Spacecraft Disintegration during Atmospheric Re-entry, Executive Summary, ESOC Contract No. 12804/98/D/IM, HTG-Report-00-4, HTG – Hyperschall Technologie Göttingen, Katlenburg-Lindau, Germany, 2000.
- Anonymous, NASA Safety Standard – Guidelines and Assessment Procedures for Limiting Orbital Debris, NSS 1740.14, NASA, Office of Safety and Mission Assurance, Washington D.C., 1995.
- Anonymous, 1990 Gridded Global Population Distribution, UNEP/GRID - Sioux Falls Dataset, United Nations Environment Programme, <http://www.na.unep.net>, 1990.